

Intermolecular Contact-Tuned Magnetic Nature in One-Dimensional 3d–5d Bimetallic Systems: From a Metamagnet to a Single-Chain Magnet

Seok Woo Choi,[†] Hyun Young Kwak,[†] Jung Hee Yoon,[†] Hyoung Chan Kim,[‡] Eui Kwan Koh,[§] and Chang Seop Hong^{*†}

Department of Chemistry, Korea University, Seoul 136-713, Korea, National Fusion Research Institute, Daejeon 305-333, Korea, and Nano-Bio System Research Team, Korea Basic Science Institute, Seoul 136-713, Korea

Received September 4, 2008

Assembling $[W(CN)_6(bpy)]^-$ and magnetic anisotropic Mn Schiff bases produced two $Mn^{III}(3d)-W^V(5d)$ bimetallic chains. Modulation of the types and degrees of interchain $\pi-\pi$ interactions in the one-dimensional coordination polymers leads to the variation of the magnetic behavior from a metamagnetic character to a single-chain magnet property.

Single-chain magnets (SCMs) show slow magnetic relaxation arising from the combined effects of intrachain magnetic interactions and single-ion anisotropy, which are found in 3d,¹ 3d–radical,² 3d–3d,³ 3d–4f,⁴ and 4f–radical systems.⁵ It is important to note that the SCM characteristic can be achieved with the condition of negligible interchain magnetic interactions compared with intrachain magnetic couplings.⁶ To construct one-dimensional (1D) structures with anisotropic nature, one of the rational strategies is to

employ both anisotropic sources and building units $[M(CN)_p(L)_q]^{n-}$ (M = paramagnetic metal ions; L = usually polydentate ligands) containing appropriate capping ligands, which preclude structural extension toward higher dimensionality. Most capped cyanometalate-based precursors reported in the literature consisted of chelating ligands with planar rings, which are beneficial to grow single crystals through the effective intermolecular $\pi-\pi$ crystal packings between the planar groups, but interchain magnetic interactions mediated through the significant intermolecular contacts are often promoted, eventually destroying a SCM property.⁷ This antagonistic propensity could serve as a hurdle of using the building blocks with aromatic rings as synthons for SCMs. We have explored the magnetic properties of 1D anisotropic chains that can be fine-tuned by intermolecular $\pi-\pi$ contacts.

We report the syntheses, structures, and magnetic characterizations of 1D chains $[W(CN)_6(bpy)][Mn(L1)] \cdot MeCN \cdot MeOH$ [**2**; bpy = 2,2'-bipyridine, $H_2L1 = N,N'$ -bis(1'-hydroxy-2'-acetophenylidene)-1,2-diaminoethane] and $[W(CN)_6(bpy)]-[Mn(L2)] \cdot H_2O$ [**3**; $H_2L2 = N,N'$ -bis(2-hydroxynaphthalene-1-carbaldehyde)-*trans*-diaminocyclohexane]. We utilized Mn Schiff bases including two fused benzene rings (naphthalene rings) with different geometric dispositions, each of which can create intermolecular stackings at various contact faces. The magnetic trait is modulated from a metamagnetic

* To whom correspondence should be addressed. E-mail: cshong@korea.ac.kr.

[†] Korea University.

[‡] National Fusion Research Institute.

[§] Korea Basic Science Institute.

- (1) Liu, T.-F.; Fu, D.; Gao, S.; Zhang, Y.-Z.; Sun, H.-L.; Su, G.; Liu, Y.-J. *J. Am. Chem. Soc.* **2003**, *125*, 13976. (b) Bernot, K.; Luzon, J.; Sessoli, R.; Vindigni, A.; Thion, J.; Richeter, S.; Leclercq, D.; Larionova, J.; Lee, A. v. d. *J. Am. Chem. Soc.* **2008**, *130*, 1619. (c) Xu, H.-B.; Wang, B.-W.; Pan, F.; Wang, Z.-M.; Gao, S. *Angew. Chem., Int. Ed.* **2007**, *46*, 7388.
- (a) Caneschi, A.; Gatteschi, D.; Lalioti, N.; Sangregorio, C.; Sessoli, R.; Venturi, G.; Vindigni, A.; Rettori, A.; Pini, M. G.; Novak, M. A. *Angew. Chem., Int. Ed.* **2001**, *40*, 1760. (b) Miyasaka, H.; Madanbashi, T.; Sugimoto, K.; Nakazawa, Y.; Wernsdorfer, W.; Sugiura, K.-i.; Yamashita, M.; Coulon, C.; Clérac, R. *Chem.—Eur. J.* **2006**, *12*, 7028.
- (a) Clérac, R.; Miyasaka, H.; Yamashita, M.; Coulon, C. *J. Am. Chem. Soc.* **2002**, *124*, 12837. (b) Pardo, E.; Ruiz-García, R.; Lloret, F.; Faus, J.; Julve, M.; Ruiz-Pérez, C. *Adv. Mater.* **2004**, *16*, 1597. (c) Pardo, E.; Ruiz-García, R.; Lloret, F.; Faus, J.; Julve, M.; Journaux, Y.; Novak, M. A.; Delgado, F. S.; Ruiz-Pérez, C. *Chem.—Eur. J.* **2007**, *13*, 2054. (d) Wang, S.; Zuo, J.-L.; Gao, S.; Song, Y.; Zhou, H.-C.; Zhang, Y.-Z.; You, X.-Z. *J. Am. Chem. Soc.* **2004**, *126*, 8900.
- (4) Costes, J.-P.; Clemente-Juan, J. M.; Dahan, F.; Milon, J. *Inorg. Chem.* **2004**, *43*, 8200.
- (5) Bogani, L.; Sangregorio, C.; Sessoli, R.; Gatteschi, D. *Angew. Chem., Int. Ed.* **2005**, *44*, 5817.

(6) Coulon, C.; Miyasaka, H.; Clérac, R. *Struct. Bonding (Berlin)* **2006**, *122*, 163.

(7) (a) Pan, F.; Wang, Z.-M.; Gao, S. *Inorg. Chem.* **2007**, *46*, 10221. (b) Jiang, L.; Feng, X.-L.; Lu, T.-B.; Gao, S. *Inorg. Chem.* **2006**, *45*, 5018. (c) Zhang, Y.-Z.; Gao, S.; Wang, Z.-M.; Su, G.; Sun, H.-L.; Pan, F. *Inorg. Chem.* **2005**, *44*, 4534. (d) Toma, L. M.; Delgado, F. S.; Ruiz-Pérez, C.; Carrasco, R.; Cano, J.; Lloret, F.; Julve, M. *Dalton Trans.* **2004**, 2836. (e) Kim, J. I.; Yoo, H. S.; Koh, E. K.; Hong, C. S. *Inorg. Chem.* **2007**, *46*, 10461. (f) Ko, H. H.; Lim, J. H.; Kim, H. C.; Hong, C. S. *Inorg. Chem.* **2006**, *45*, 8847. (g) Yoon, J. H.; Lim, J. H.; Choi, S. W.; Kim, H. C.; Hong, C. S. *Inorg. Chem.* **2007**, *46*, 1529. (h) Wen, H.-R.; Wang, C.-F.; Song, Y.; Gao, S.; Zuo, J.-L.; You, X.-Z. *Inorg. Chem.* **2006**, *45*, 8942.

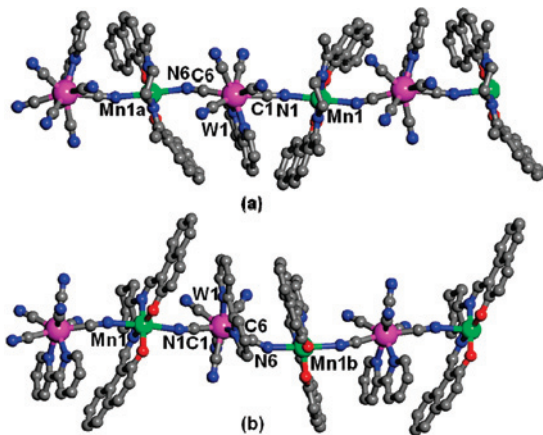
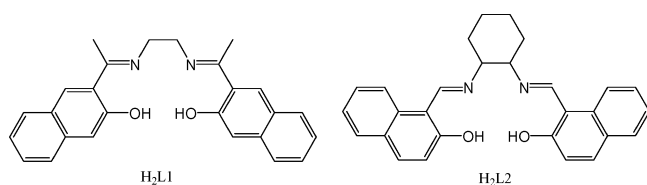


Figure 1. Molecular views of **2** (a) and **3** (b). Symmetry transformations used to generate equivalent atoms: $a = -0.5 + x, 1.5 - y, 0.5 + z$; $b = x, 1 - y, 0.5 + z$.

character in **2** to a SCM property in **3**, which marks the first SCM example involving 5d metal ions.



A stoichiometric reaction of $[\text{W}(\text{CN})_6(\text{bpy})]^- (\mathbf{1})^8$ with the Mn Schiff bases⁹ afforded deep-brown crystals of **2** and **3**.¹⁰ The characteristic CN peaks in the IR spectra are centered at 2171w, 2159w, 2152vw, 2134w (sh), and 2115w cm^{-1} for **2** and 2148w, 2139w (sh), and 2118w cm^{-1} for **3**. Some peaks in **2** shift toward higher frequencies based on the IR peaks of the precursor (**1**) visible at 2146w, 2135w, and 2119w cm^{-1} , suggesting the existence of bridging CN ligands. However, the observed peaks in **3** are close to those in **1**, implying that the coordination of the N end in the CN group to a metal center is somewhat weak, if existing at all.

In the crystal structures [Figures S1 (Supporting Information) and 1], the central environments of W belong to a distorted dodecahedron for **1** and a distorted square antiprism for **2** and **3** (Table S1 in the Supporting Information). Two groups among the six CN ligands of the $\text{W}(\text{CN})_6(\text{bpy})^-$ moiety behave as bridges to Mn Schiff bases, generating a 1D linear chain structure. The Mn^{III} center adopts a distorted

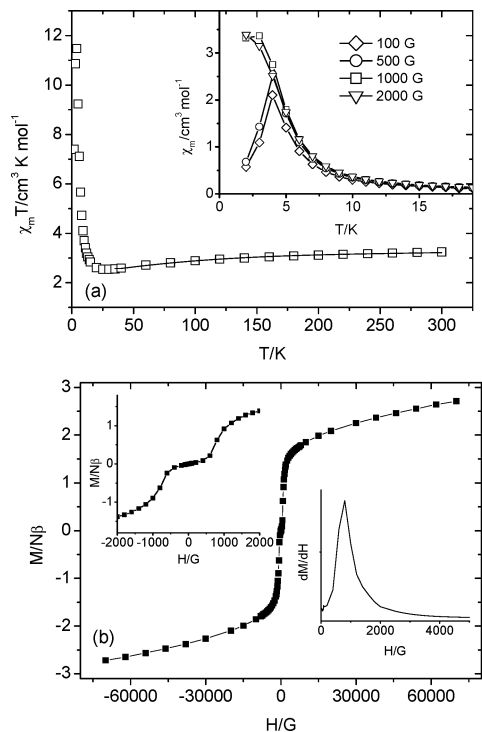


Figure 2. (a) Plots of $\chi_m T$ and χ_m (inset) vs T for **2**. The solid line in the main panel shows the best fit to the magnetic model. (b) Field dependence of M at 2 K for **2**.

octahedral arrangement with a significant tetragonal elongation. The axial Mn–N distances [Mn1–N1 = 2.294(4) Å and Mn1a–N6 = 2.311(3) Å for **2**, $a = -0.5 + x, 1.5 - y, 0.5 + z$; Mn1–N1 = 2.438(4) Å and Mn1b–N6 = 2.371(4) Å for **3**, $b = x, 1 - y, 0.5 + z$] are longer than the average equatorial Mn–N(O) lengths [1.93(7) Å for **2** and 1.93(5) Å for **3**]. There exist two different Mn–N–C(cyanide) angles within a chain [Mn1–N1–C1 = 165.0(3)° and Mn1a–N6–C6 = 153.9(3)° for **2** and Mn1–N1–C1 = 163.8(4)° and Mn1b–N6–C6 = 156.0(4)° for **3**]. The average Mn–N–C angles are quite akin to each other. The intrachain metal–metal separations through the CN bridges are W1–Mn1 of 5.5513(5) Å, W1–Mn1a of 5.4764(5) Å for **2**, and W1–Mn1 of 5.6937(7) Å and W1–Mn1b of 5.5582(8) Å for **3**. Hydrogen bonding is formed between O atoms of methanols and one of free N atoms of cyanides for **2**.

The π – π contacts with a centroid distance of 3.859 Å are formed through phenoxide rings of L1 in **2**, whereas rather weak intermolecular interactions with a centroid distance of 3.933 Å are established between phenoxide and benzene rings of L2 in **3** (Figures S2 and S3 in the Supporting Information). Accordingly, the interchain magnetic routes through the π – π -stacking interactions for **3** are relatively longer than those for **2** because of the involvement of the different aromatic rings in the formation of such noncovalent forces. The shortest interchain Mn–Mn distance (9.547 Å) through the intermolecular forces between the disparate planar rings on the naphthyl groups for **2** is much shorter than that (10.664 Å) for **3**.

The magnetic data are plotted in Figures 2 and 3. As the temperature is lowered, the $\chi_m T$ product decreases slowly down to a minimum at $T_{\text{min}} = 30$ K for **2** and 20 K for **3**.

(8) Szklarzewicz, J. *Inorg. Chim. Acta* **1993**, *205*, 85.

(9) Miyasaka, H.; Clérac, R.; Ishii, T.; Chang, H.-C.; Kitagawa, S.; Yamashita, M. *J. Chem. Soc., Dalton Trans.* **2002**, 1528.

(10) Crystal data of **1**: $M_r = 1691.08$, triclinic, space group $P\bar{1}$, $a = 9.2764(17)$ Å, $b = 14.473(3)$ Å, $c = 14.995(3)$ Å, $\alpha = 113.034(6)^\circ$, $\beta = 97.370(6)^\circ$, $\gamma = 97.220(6)^\circ$, $V = 1803.0(6)$ Å³, $Z = 1$, $D_{\text{calc}} = 1.557$ g cm^{-3} , $\mu = 3.290$ mm⁻¹, 19 289 reflections collected, 8094 unique ($R_{\text{int}} = 0.0763$), $R1 = 0.0473$, $wR2 = 0.0648$ [$I > 2\sigma(I)$]. Crystal data of **2**: $M_r = 1018.65$, monoclinic, space group $P2_1/n$, $a = 14.5410(3)$ Å, $b = 19.3159(5)$ Å, $c = 14.9197(3)$ Å, $\beta = 94.1540(10)^\circ$, $V = 4179.52(16)$ Å³, $Z = 4$, $D_{\text{calc}} = 1.619$ g cm^{-3} , $\mu = 3.108$ mm⁻¹, 76 031 reflections collected, 10 384 unique ($R_{\text{int}} = 0.0784$), $R1 = 0.0349$, $wR2 = 0.0540$ [$I > 2\sigma(I)$]. Crystal data of **3**: $M_r = 989.60$, monoclinic, space group $C2/c$, $a = 39.3224(8)$ Å, $b = 10.6638(2)$ Å, $c = 22.0184(5)$ Å, $\beta = 121.6070(10)^\circ$, $V = 7863.3(3)$ Å³, $Z = 8$, $D_{\text{calc}} = 1.672$ g cm^{-3} , $\mu = 3.300$ mm⁻¹, 38 572 reflections collected, 9745 unique ($R_{\text{int}} = 0.0603$), $R1 = 0.0377$, $wR2 = 0.0721$ [$I > 2\sigma(I)$].

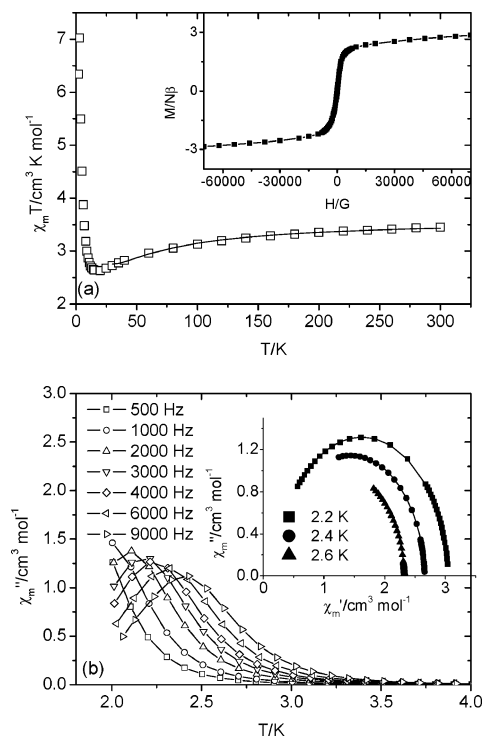


Figure 3. (a) Temperature and field dependences (inset) of magnetic data for **3**. The solid line in the main panel presents the best fit to the magnetic model. (b) Out-of-phase ac data and Cole–Cole plots (inset) for **3** at indicated frequencies and temperatures, respectively.

Below T_{\min} , $\chi_m T$ undergoes an abrupt rise to a cusp at $T_{\max} = 4$ K for **2** and 3 K for **3**. These behaviors are associated with the operation of antiferromagnetic interactions between $S_{\text{Mn}} = 2$ and $S_{\text{W}} = 1/2$. The fit of an analytical expression derived by Drillon et al.¹¹ to the data in the temperature ranges of 35–300 K (**2**) and 30–300 K (**3**) affords estimated results of $g_{\text{Mn}} = 2.00$, $g_{\text{W}} = 2.15$, and $J = -15.2$ cm⁻¹ for **2** and $g_{\text{Mn}} = 2.06$, $g_{\text{W}} = 2.14$, and $J = -11.8$ cm⁻¹ for **3**.¹² The stronger J value in **2** than in **3** can be understood by the structural parameters that the mean Mn–N(cyanide) length in **2** is significantly shorter than that in **3**, whereas the average Mn–N–C angles remain alike.

The $M(H)$ data of **2** show a regular metamagnetic behavior with a critical field of 800 G determined by the derivative of M with respect to H (Figure 2). Below this field, interchain magnetic interactions are dominant, as judged by peaks at 4 K in the $\chi_m(T)$ plots. The antiferromagnetic couplings between neighboring chains originate from the π – π contacts of the phenoxide groups. Application of a magnetic field higher than 800 G enables the weak interchain interactions to be overcome and brings about a phase transition from the antiferromagnetic state to a ferrimagnetic state. The experimental value of $2.71 N\beta$ at 7 T is comparable to the expected ferrimagnetic value for $gS = gS_{\text{Mn}} - gS_{\text{W}} = 3 N\beta$, assuming $g = 2$. Strikingly, however, the metamagnetic phenomenon

in **2** disappears in **3**, where a ferrimagnetic state is also stabilized with a saturation magnetization of $2.85 N\beta$ at 7 T (inset of Figure 3a). This implies that the π – π stackings through L2 in **3** transmit very weak or virtually negligible magnetic couplings compared with L1 in **2**. To further inspect the underlying magnetic property of **3**, alternating current (ac) magnetic susceptibility data were collected at a zero direct current field and an ac field of 5 G [Figures 3b and S4 (Supporting Information)]. The maxima at T_p in χ_m' move toward higher temperatures with increasing oscillating frequency (f). A quantity given by $\Delta T_p/[T_p \Delta(\log f)]$ is estimated to be 0.20, which falls in the range of a superparamagnet.^{1–6,13} The Arrhenius equation of $\tau = \tau_0 \exp(\Delta_\tau/kT)$, where $\tau = 1/2\pi f$, was employed to extract parameters relevant with a slow magnetic relaxation. A best fit of peak temperatures in χ_m'' to the equation affords $\tau_0 = 3.9 \times 10^{-10}$ s, which is consistent with observed values of SCMs (Figure S5 in the Supporting Information),^{1–6} and $\Delta_\tau/k = 25.8$ K. On the basis of the Glauber model, the correlation length (ξ) diverges exponentially in a ferrimagnetic 1D anisotropic system, which can be described as the expression of $\chi T = C_{\text{eff}} \exp(\Delta_\xi/kT)$, where Δ_ξ is the energy barrier to create a domain wall in the chain.^{6,14} A linear fit of $\ln(\chi_m' T)$ against $1/T$ gives $\Delta_\xi/k = 3.6$ K, ensuring the 1D Ising chain in **3** (Figure S6 in the Supporting Information). The low-temperature maximum in the curve is concerned with finite size effects, and the limitation of growing the correlation length is due to the presence of structural defects on the chains.¹⁵ The Cole–Cole plots (inset of Figure 3b), measured at temperatures of 2.2, 2.4, and 2.6 K, provide a semicircle, and fitting with a generalized Debye model leads to values of α of less than 0.057.¹⁵ The α parameters reveal a substantially narrow distribution of relaxation times, which are typical for reported SCMs.^{1–5}

In summary, we have prepared and characterized two bimetallic chains constructed by $[\text{W}(\text{CN})_6(\text{bpy})]^-$ and magnetic anisotropic Mn Schiff bases. The magnetic properties are altered from a metamagnet (**2**) to a SCM (**3**), marking the first case of the SCM with 3d–5d metal centers. The variation of the magnetic behaviors relies on the types and degrees of fine-tuned interchain π – π interactions.

Acknowledgment. This work was supported by a Korea Science and Engineering Foundation (KOSEF) grant (Grant R01-2007-000-10240-0).

Supporting Information Available: X-ray crystallographic files in CIF format and additional synthetic, structural, and magnetic data for **1–3**. This material is available free of charge via the Internet at <http://pubs.acs.org>.

IC801699P

(11) Drillon, M.; Coronado, E.; Beltran, D.; Georges, R. *Chem. Phys.* **1983**, *79*, 449.

(12) Given that Mn^{III} and W^V spins are antiparallel, Mn^{III} was assumed to act as a classical spin carrier with $S_{\text{Mn}} = 2$, leading to an effective alternating chain with $S_{\text{Mn}} = 2$ and $S_{\text{W}} = 1/2$. The magnetic model may be roughly applied to the system with the quantum spin $S_{\text{W}} = 1/2$.

(13) Mydosh, J. A. *Spin Glasses: An Experimental Introduction*; Taylor & Francis: London, 1993.

(14) Coulon, C.; Clérac, R.; Lecren, L.; Wernsdorfer, W.; Miyasaka, H. *Phys. Rev. B* **2004**, *69*, 132408.

(15) Aubin, S. M. J.; Sun, Z.; Pardi, L.; Krzystek, J.; Folting, K.; Brunel, L.-C.; Rheingold, A. L.; Christou, G.; Hendrickson, D. N. *Inorg. Chem.* **1999**, *38*, 5329.